Mon. Not. R. Astron. Soc. **329,** 572–578 (2002)

Radiation drag driven mass accretion in a clumpy interstellar medium: implications for the supermassive black hole-to-bulge relation

Nozomu Kawakatu★ and Masayuki Umemura★
Centre for Computational Physics, University of Tsukuba, Tsukuba, Ibaraki 305, Japan

Accepted 2001 September 20. Received 2001 August 17; in original form 2001 May 30

ABSTRACT

We quantitatively scrutinize the effects of the radiation drag arising from the radiation fields in a galactic bulge in order to examine the possibility that the radiation drag could be an effective mechanism to extract angular momentum in a spheroidal system like a bulge and allow plenty of gas to accrete on to the galactic centre. For this purpose, we numerically solve the relativistic radiation hydrodynamical equation coupled with accurate radiative transfer, and quantitatively assess the radiation drag efficiency. As a result, we find that in an optically thick regime the radiation drag efficiency is sensitively dependent on the density distributions of the interstellar medium (ISM). The efficiency drops according to τ_{T}^{-2} in an optically thick *uniform* ISM, where τ_{T} is the total optical depth of the dusty ISM, whereas the efficiency remains almost constant at a high level if the ISM is *clumpy*. Hence, if bulge formation begins with a star formation event in a clumpy ISM, the radiation drag will effectively work to remove the angular momentum and the accreted gas may form a supermassive black hole. As a natural consequence, this mechanism reproduces a putative linear relation between the mass of a supermassive black hole and the mass of a galactic bulge, although further detailed modelling for stellar evolution is required for a more precise prediction.

Key words: galaxies: bulges – galaxies: nuclei – galaxies: starburst.

1 INTRODUCTION

Recently, Kormendy & Richstone (1995) have pioneeringly suggested that the mass of a supermassive black hole (BH) does correlate linearly with the mass of the host bulge. (It is noted that the term ‘bulge’ is used to mean a whole galaxy for an elliptical galaxy in this paper, as is often so.) Further high-quality observations of the galactic centre using stellar dynamics, gas dynamics and maser dynamics (Miyoshi et al. 1995; Magorrian et al. 1998; Richstone et al. 1998; Ho 1999; Wandel 1999; Kormendy & Ho 2000; Gebhardt et al. 2000b; Ferrarese et al. 2001; Sarzi et al. 2001; Merritt & Ferrarese 2001a) allow us to make a detailed demography of supermassive BHs. The recent findings are the following. (1) The BH mass exhibits a linear relation to the bulge mass for a wide range of BH mass with a median BH mass fraction of $f_{\mathrm{BH}} \equiv M_{\mathrm{BH}}/M_{\mathrm{bulge}} = 0.001-0.006$ (Kormendy & Richstone 1995; Richstone et al. 1998; Magorrian et al. 1998; Gebhardt et al. 2000b; Ferrarese & Merritt 2000; Merritt & Ferrarese 2001a). (2) The BH mass correlates with the velocity dispersion of bulge stars with a power-law relation as $M_{\mathrm{BH}} \propto \sigma^n$, $n = 3.75$ (Gebhardt et al. 2000a) or 4.72 (Ferrarese & Merritt 2000; Merritt & Ferrarese 2001a,b). (3) f_{BH} tends to grow with the age of the youngest stars in a bulge until 10^9 yr (Merrifield, Forbes & Terlevich 2000). (4) In disc galaxies, the mass ratio is significantly smaller than 0.001 if the disc stars are included (Salucci et al. 2000; Sarzi et al. 2001). (5) For quasars, f_{BH} is on a similar level to that for elliptical galaxies (Laor 1998; Mclure & Dunlop 2001a; Wandel 2001). (6) f_{BH} in Seyfert 1 galaxies is under debate, and may be considerably smaller than 0.001 (Wandel 1999; Gebhardt et al. 2000b) or similar to that for ellipticals (McLure & Dunlop 2001a,b; Wandel 2001), while the BH mass-to-velocity dispersion relation in Seyfert 1 galaxies seems to hold good in a similar way to elliptical galaxies (Gebhardt et al. 2000a; Nelson 2000; Ferrarese et al. 2001). These BH-to-bulge correlations suggest that the formation of a supermassive BH is physically connected with the formation of a galactic bulge.

So far, very little is understood about the physical mechanism to produce such correlations, although some theoretical models have been proposed (Silk & Rees 1998; Ostriker 2000; Adams, Graff & Richstone 2001). Recently, as a possible mechanism to work in a spheroidal system, Umemura (2001) has considered the effects of radiation drag. The radiation drag is a relativistic effect, which may extract angular momentum effectively in a spheroidal system like a bulge, so that plenty of interstellar medium (ISM) could accrete on to the galactic centre. Obviously, the radiation drag is inefficient in present-day elliptical galaxies or galactic bulges, since they

★E-mail: kawakatu@rccp.tsukuba.ac.jp (NK); umemura@rccp.tsukuba.ac.jp (MU)

possess little ISM. If the contents of a supermassive BH are initially in the form of ISM, however, the bulge must have been optically thick in the early stage:

$$\tau \approx \chi\rho r_{\mathrm{b}} = 1.0\left(\frac{\chi}{100\,\mathrm{cm}^2\,\mathrm{g}^{-1}}\right)\left(\frac{M_{\mathrm{gas}}}{10^9\,\mathrm{M}_{\odot}}\right)\left(\frac{r_{\mathrm{b}}}{3\,\mathrm{kpc}}\right)^{-2},$$

where χ is the mass extinction coefficient due to dust opacity of the ISM, M_{gas} is the mass of the ISM, and r_{b} is the bulge radius. If a considerable amount of gas is expelled by a galactic wind at some stage, the optical depth should be still larger before the wind. If the radiation drag works efficiently in an optically thick medium, the rate of mass accretion induced by the radiation drag is maximally L_{bol}/c^2 (Umemura, Fukue & Mineshige 1997, 1998; Fukue, Umemura & Mineshige 1997), where L_{bol} is the bolometric luminosity. Umemura (2001) has found that, if the maximal drag efficiency is achieved, the resultant BH-to-bulge mass ratio is basically determined by the energy conversion efficiency of the nuclear fusion from hydrogen to helium, i.e. 0.007. However, it is not very clear whether this mechanism really works efficiently in realistic situations.

In this paper, we investigate in detail the efficiency of the radiation drag in an optically thick ISM to test whether the radiation drag model is promising to account for the putative BH-to-bulge correlations. In particular, we concentrate our attention on the effects of the inhomogeneity in the ISM. The model for the chemical evolution of elliptical galaxies suggests that an elliptical galaxy is initiated by a starburst in its early stages (10^7 yr) and evolves passively after a galactic wind event at a few $\times 10^8$ yr (Arimoto & Yoshii, 1986, 1987; Kodama & Arimoto, 1997; Mori et al. 1997). Also, in nearby starburst galaxies that have been studied, the ISM is highly clumpy (Sanders et al. 1988; Gordon, Calzetti & Witt 1997). Thus, if we consider the radiation drag in the early phase of bulge evolution, we should consider an inhomogeneous optically thick ISM. In this paper, to elucidate the mutual effect between the clumpiness of the ISM and the optical depth on the radiation drag efficiency, we build up a simple model of the bulge system and accurately solve the radiation transfer in a clumpy ISM.

The paper is organized as follows. In Section 2, we construct the model of a galactic bulge. In Section 3, the basic equations for the ISM are provided. In Section 4, the angular momentum transfer efficiency is assessed in a *uniform* ISM. In Section 5, we investigate the angular momentum transfer efficiency by solving the radiation transfer in a *clumpy* ISM, and elucidate the relationship between the clumpiness of the ISM and the angular momentum transfer efficiency. In Section 6, we give implications for the correlation between the supermassive BH mass and the bulge mass. In addition, we discuss further effects that would have significant influence on the BH mass. Section 7 is devoted to our conclusions.

2 MODEL

We assume that a spherical galactic bulge consists of three components, that is, dark matter, stars and a dusty ISM. The bulge radius r_{b} is set to be 1–10 kpc by taking account of the observed sizes of elliptical galaxies or bulges in spiral galaxies. Dark matter is distributed uniformly inside the bulge. The mass of the dark matter component, M_{DM}, within the bulge is equal to the stellar mass of the galactic bulge, M_{bulge}. As for the stellar component, we assume star clusters with a specific stellar initial mass function (see below). The star clusters are distributed uniformly inside the galactic bulge. Hereafter, ‘a star’ in this paper means ‘a star cluster’. Here, N_* ($=100$) stars are distributed randomly. For a dusty ISM, we consider two cases: one is a uniformly distributed ISM, and the other is a clumpy ISM. In the case of a clumpy ISM, N_{c} ($=10^4$) identical clouds are distributed randomly. The density ρ_{gas} in a cloud is assumed to be uniform. The size of a gas cloud, r_{c}, is a parameter. Then, the optical depth of a gas cloud is $\bar{\tau} = \chi\rho_{\mathrm{gas}}r_{\mathrm{c}}$, where χ is the mass extinction. We suppose that the stars and the ISM clouds corotate with angular velocity corresponding to the angular momentum obtained by the tidal torque at the linear stage of density fluctuations. Quantitatively, the angular momentum is given by the spin parameter $\lambda = (J_{\mathrm{T}}|E_{\mathrm{T}}|^{1/2})/(GM_{\mathrm{T}}^{5/2}) = 0.05$, where J_{T}, E_{T} and M_{T} are respectively the total angular momentum, energy and mass (Barns & Efstathiou 1987; Heavens & Peacock 1988). Here, rigid rotation is assumed.

The mass range of galactic bulges is postulated to be $10^{6-13}\,\mathrm{M}_{\odot}$. (However, in the present analysis, it is not very important to specify M_{bulge}, because the results are scaled with M_{bulge} as shown below.) The total mass of the ISM, M_{gas}, and the mass of each gas cloud, m_{c}, are parameters. If dust opacity as well as Thomson scattering is considered, the mass extinction is expressed by $\chi = (n_{\mathrm{e}}\sigma_{\mathrm{T}} + n_{\mathrm{d}}\sigma_{\mathrm{d}})/(\rho_{\mathrm{g}} + \rho_{\mathrm{d}})$, where σ_{T} is the Thomson scattering cross-section, n_{e} is the electron number density, ρ_{g} is the gas density, and n_{d}, σ_{d} and ρ_{d} are respectively the number density, cross-section and mass density of dust grains. If we take a dust-to-gas mass ratio f_{dg} of $\sim 10^{-2}$, then the opacity ratio is

$$\frac{n_{\mathrm{d}}\sigma_{\mathrm{d}}}{n_{\mathrm{e}}\sigma_{\mathrm{T}}} = 1.9 \times 10^2\left(\frac{a_{\mathrm{d}}}{1\,\mu\mathrm{m}}\right)^{-1}\left(\frac{\rho_{\mathrm{s}}}{\mathrm{g\,cm}^{-3}}\right)^{-1}\left(\frac{f_{\mathrm{dg}}}{10^{-2}}\right),$$

where a_{d} is the grain radius and ρ_{s} is the density of solid material within the grain. Thus we find $n_{\mathrm{d}}\sigma_{\mathrm{d}} \gg n_{\mathrm{e}}\sigma_{\mathrm{T}}$ in the situations of interest. Hence, in this paper, we evaluate the mass extinction by $\chi = n_{\mathrm{d}}\sigma_{\mathrm{d}}/\rho_{\mathrm{g}}$.

Finally, as for stellar evolution, we assume a Salpeter-type initial mass function (IMF) as $\phi = A(m_*/\mathrm{M}_{\odot})^{-1.35}$ for a mass range of $[m_{\mathrm{l}}, m_{\mathrm{u}}]$. In the present analysis, we consider an initial starburst and the subsequent passive evolution of stars. The upper mass limit is inferred to be around $40\,\mathrm{M}_{\odot}$ in starburst regions (Doyon, Puxley & Joseph 1992). As for the lower mass limit, some authors suggest that the IMF in starburst regions is deficient in low-mass stars, with a cut-off of about $2-3\,\mathrm{M}_{\odot}$ (Doane & Mathews 1993; Charlot et al. 1993; Hill et al. 1994). In this paper, we assume $m_{\mathrm{l}} = 2\,\mathrm{M}_{\odot}$ and $m_{\mathrm{u}} = 40\,\mathrm{M}_{\odot}$ in the early stages of bulge formation. However, it should be also kept in mind that the lower mass limit is under debate; the claimed lower cut-off could be due to the magnitude limit effect (Selman et al. 1999), and also recently sub-solar-mass stars have been found in the starburst region in our Galaxy, NGC 3603 (Brandl et al. 1999). In order to incorporate the stellar evolution, we adopt the mass–luminosity relation $(\ell_*/\mathrm{L}_{\odot}) = (m_*/\mathrm{M}_{\odot})^{3.7}$, and the mass–age relation $\tau_* = 1.1 \times 10^{10}(m_*/\mathrm{M}_{\odot})^{-2.7}$ yr (Lang 1974), where m_*, ℓ_* and τ_* are respectively the stellar mass, luminosity and age.

3 BASIC EQUATIONS

As a relativistic result of radiative absorption and subsequent re-emission, the radiation fields exert a drag force on moving material in resistance to its velocity. This radiation drag extracts angular momentum from the ISM, thereby allowing the gas to accrete on to the galactic centre. The radiation drag is an effect of $O(v/c)$, but it could provide a key mechanism for angular momentum transfer in intense radiation fields. We put the origin at the centre of the bulge, and adopt cylindrical coordinates r, ϕ and z, where the z-axis is the rotation axis of stars and gas. The components of the specific radiation force that is exerted on moving fluid elements with velocity $\boldsymbol{v}$ are given by

$$f_r = \frac{\chi}{c}(F^r - v_r E - v_r P^{rr} - v_\phi P^{\phi r} - v_z P^{zr}), \tag{1}$$

$$f_\phi = \frac{\chi}{c}(F^\phi - v_\phi E - v_\phi P^{\phi\phi} - v_r P^{r\phi} - v_z P^{z\phi}) \tag{2}$$

and

$$f_z = \frac{\chi}{c}(F^z - v_z E - v_z P^{zz} - v_r P^{rz} - v_\phi P^{\phi z}) \tag{3}$$

(Mihalas & Mihalas 1984) in the r-, ϕ-, and z-directions respectively. Here, E is the radiation energy density, F^α is the radiation flux, and $P^{\alpha\beta}$ is the radiation stress tensor where the non-diagonal components are null owing to the present symmetry.

Using equations (1)–(3), we have the radiation hydrodynamical equations to $O(v/c)$ as

$$\frac{\mathrm{d}v_r}{\mathrm{d}t} = \frac{v_\phi^2}{r} - f_{\mathrm{g}}^r + \frac{\chi}{c}[F^r - (E + P^{rr})v_r], \tag{4}$$

$$\frac{1}{r}\frac{\mathrm{d}(rv_\phi)}{\mathrm{d}t} = \frac{\chi}{c}[F^\phi - (E + P^{\phi\phi})v_\phi], \tag{5}$$

$$\frac{\mathrm{d}v_z}{\mathrm{d}t} = -f_{\mathrm{g}}^z + \frac{\chi}{c}[F^z - (E + P^{zz})v_z], \tag{6}$$

where f_{g}^r and f_{g}^z are respectively the r- and z-components of the gravitational force.

The azimuthal equation of motion (5) is the equation of angular momentum transfer. This equation implies that the radiation flux force (the first term on the right-hand side) makes fluid elements tend to corotate with stars, whereas the radiation drag (the second term on the right-hand side) works to extract the angular momentum from gas. Therefore the gain and loss of total angular momentum are determined by equation (5).

4 UNIFORM ISM

In this section, we consider the angular momentum transfer by radiation drag in a uniform ISM. First, we analytically calculate the radiation fields produced by spherically distributed stars in an optically thin regime, and assess the angular momentum loss rate $\dot{J}$ and the mass accretion rate $\dot{M}$. Next, we extend the analysis to an optically thick regime. Then the relationship between the optical depth of a dusty ISM and the angular momentum transfer efficiency is derived.

4.1 Optically thin regime

For uniform distributions of stars, the radiation fields inside the bulge are analytically integrated in an optically thin regime to be

$$cE = \frac{3L_{\mathrm{bulge}}}{2\pi r_{\mathrm{b}}^2}\left(1 - \frac{\pi}{4}\frac{r}{r_{\mathrm{b}}}\right), \tag{7}$$

$$F^r = \frac{L_{\mathrm{bulge}}}{4\pi r_{\mathrm{b}}^3} r, \tag{8}$$

$$cF^\phi = \frac{3L_{\mathrm{bulge}}}{2\pi r_{\mathrm{b}}^2}\omega r_{\mathrm{b}}\left(\frac{215}{216} - \frac{49\pi}{192}\right) \times \left(\frac{r}{r_b}\right)^2 + \frac{3L_{\mathrm{bulge}}}{2\pi r_{\mathrm{b}}^2}\omega r_{\mathrm{b}}\frac{8}{9}\frac{r}{r_{\mathrm{b}}}\left(1 - \frac{r}{r_{\mathrm{b}}}\right), \tag{9}$$

$$F^z = \frac{L_{\mathrm{bulge}}}{4\pi r_{\mathrm{b}}^3} z, \tag{10}$$

$$cP^{rr} = \frac{1}{3}\frac{3L_{\mathrm{bulge}}}{2\pi r_{\mathrm{b}}^2}\left(1 - \frac{3\pi}{16}\frac{r}{r_{\mathrm{b}}}\right), \tag{11}$$

$$cP^{\phi\phi} = \frac{1}{3}\frac{3L_{\mathrm{bulge}}}{2\pi r_{\mathrm{b}}^2}\left(1 - \frac{9\pi}{32}\frac{r}{r_{\mathrm{b}}}\right), \tag{12}$$

$$cP^{zz} = cP^{\phi\phi}, \tag{13}$$

where L_{bulge} and r_{b} are the luminosity and radius of the bulge and ω is the angular velocity of stars. These quantities are equivalent to those obtained by Fukue et al. (1997), except that the radiation flux F^ϕ in the azimuthal direction is generated by the rotation of the bulge. As seen in equation (5), the flux F^ϕ works to corotate the ISM with stars, in contrast to the drag force. In Fig. 1, we compare both forces exerted on gas per unit mass, $f^{\mathrm{drag}}\chi(E + P^{\phi\phi})v_\phi/c$ and $f^\phi = \chi F^\phi/c$, where $v_\phi = r\omega$. It is found that f^{drag} overwhelms f^ϕ everywhere. Thus the optically thin ISM can always lose angular momentum as a result of radiation drag. The angular momentum loss rate per unit volume per unit time $\dot{j}$ is evaluated by

$$\dot{j} = -\frac{L_{\mathrm{bulge}}}{c^2}\frac{3\chi\omega}{2\pi}xf(x) \tag{14}$$

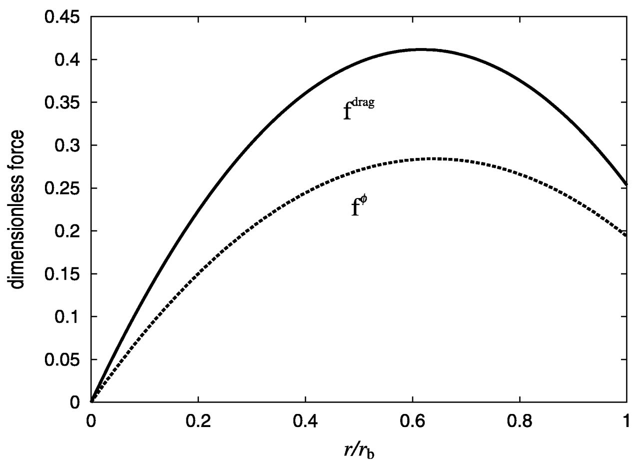

Figure 1. The radiation drag force f^{drag} is compared with the flux force f^ϕ in the azimuthal direction. The x-axis is the radial distance normalized by the bulge radius r_{b}, and the radiation force is normalized by $(3\chi\omega L_{\mathrm{bulge}})/(2\pi c^2 r_{\mathrm{b}})$. The figure shows that f^{drag} overwhelms f^ϕ everywhere.

at the point $x = r/r_b$, where

$$f(x) = \left(\frac{23}{216} + \frac{17\pi}{192}\right)x^2 + \frac{4}{9}x.$$

Equation (14) is integrated over the volume of the bulge to give the total angular momentum loss rate $\dot{J}$ as

$$\dot{J} = -\beta \frac{L_{\rm bulge}}{c^2}\frac{3\chi\omega}{2\pi} r_b^3 \rho_0, \tag{15}$$

where ρ_0 is the density of the ISM, and $\beta = \int x f(x)\,{\rm d}V$ with ${\rm d}V$ being the volume element in spherical coordinates. Noting that the initial angular momentum is

$$J_0 = \frac{2}{5} M_{\rm gas}\omega r_b^2, \tag{16}$$

the mass accretion rate is expressed as

$$\dot{M}_{\rm gas} = -M_{\rm gas}\frac{\dot{J}}{J_0} = \eta \frac{L_{\rm bulge}}{c^2}\tau_{\rm T}, \tag{17}$$

where $\tau_{\rm T} = \chi\rho_0 r_b = (3\chi M_{\rm gas})/(4\pi r_b^2)$. The coefficient η gives the radiation drag efficiency. By calculating the constant β numerically, η is found to be 0.32.

4.2 Optically thick regime

In the optically thick ISM, the regions where the optical depth τ_s from each star is less than unity are subject to radiation drag (Tsuribe & Umemura 1997). In this situation, the flux for the region of $\tau_s \le 1$ is given by

$$F^{\phi} = \int ER\omega\,{\rm d}V, \tag{18}$$

and

$$F^{\rm drag} = \int (E + P^{\phi\phi}) R_g \omega\,{\rm d}V \simeq \int E R_g\omega\,{\rm d}V, \tag{19}$$

where R are R_g are respectively the distance from the rotational axis to a star and to one volume element, and ${\rm d}V = r^2\sin\theta\,{\rm d}r\,{\rm d}\theta\,{\rm d}\phi$ in spherical coordinates for the position of a star. $E = \ell_*/4\pi c r^2, P^{\phi\phi} \simeq 0$ with ℓ_* being the luminosity of a star. Consequently, the local angular momentum transfer rate by equation (5) is

$$\dot{j} = -\frac{\ell_*}{c^2}\frac{\chi\omega}{6} r_s^3\rho_0. \tag{20}$$

This is summed up over all stars to give

$$\dot{J} = -\frac{1}{6}\frac{L_{\rm bulge}}{c^2}\chi\omega r_s^3\rho_0, \tag{21}$$

where r_s is the size of the region of $\tau_s = 1$, and $L_{\rm bulge} = N_*\ell_*$. Then the mass accretion rate is given as

$$\dot{M}_{\rm gas} = -M_{\rm gas}\frac{\dot{J}}{J_0}\frac{5}{12} = \frac{L_{\rm bulge}}{c^2}\tau_{\rm T}^{-2}. \tag{22}$$

So far, we have considered a rigidly rotating system. We can also analytically estimate the accretion rate in a system with a different rotation law as $v_\phi \sim r^n$ (e.g. $n = -0.5$ for Keplerian rotation). Then the mass accretion rate turns out to be

$$\dot{M}_{\rm gas} = -M_{\rm gas}\frac{\dot{J}}{J_0} = \frac{n^2(n+4)}{9B}\left(\frac{\bar{R}_i}{r_b}\right)^{n-1}\frac{L_{\rm bulge}}{c^2}\tau_{\rm T}^{-2}, \tag{23}$$

where

$$B = \sqrt{\pi}\,\Gamma\left(\frac{n+3}{2}\right)/\Gamma\left(\frac{n+4}{2}\right),$$

$\bar{R}_i$ is the mean distance from the rotational axis to each star, and $\Gamma(n)$ is the Gamma function. It is noted that the difference between (22) and (23) is merely a small factor for ordinary rotation laws. As a result, it is found that the mass accretion rate decreases according to $\tau_{\rm T}^{-2}$ in an optically thick regime. The physical reason is that the larger is the optical depth of the bulge, the closer to zero is the difference between the velocity of stars and the gas velocity, so that the radiation drag efficiency falls.

Combined with the optically thin case, we have the mass accretion rate in the uniform case as

$$\dot{M}_{\rm gas} \propto \begin{cases} \frac{L_{\rm bulge}}{c^2}\tau_{\rm T} & (\tau_{\rm T} < 1), \\ \frac{L_{\rm bulge}}{c^2}\tau_{\rm T}^{-2} & (\tau_{\rm T} > 1). \end{cases} \tag{24}$$

As readily understood by these results, the angular momentum transfer efficiency by the radiation drag is a maximum when the optical depth of the ISM is around unity.

5 CLUMPY ISM

In the previous section, we considered the angular momentum transfer in a uniform ISM. In this section, we consider a clumpy ISM. First, we describe the treatment for extinction by clumpy gas clouds. Next, by solving the radiative transfer numerically, we assess the total angular momentum loss rate $\dot{J}$ and the mass accretion rate $\dot{M}_{\rm gas}$. Then we elucidate the relation between the clumpiness of the ISM and the angular momentum transfer efficiency quantitatively.

5.1 Extinction by a clumpy ISM

In the case of a clumpy ISM, N_c (=10^4) identical clouds with an optical depth of $\bar{\tau} = \chi\rho_{\rm gas} r_c$ are distributed randomly. In an optically thin regime, the radiation fields produced by a star are

$${\rm d}E_0 = \frac{1}{c}\frac{\ell_*}{4\pi r^2}, {\rm d}\boldsymbol{F}_0 = \frac{\ell_*}{4\pi r^3}\boldsymbol{r}, {\rm d}P_0^{rr} = {\rm d}E_0, {\rm d}P_0^{\phi\phi} = {\rm d}P_0^{zz} \simeq 0, \tag{25}$$

where $\boldsymbol{r} = \boldsymbol{r}_i - \boldsymbol{r}_j$ and $r = |\boldsymbol{r}|$ with $\boldsymbol{r}_i$ being the position of the ith cloud and $\boldsymbol{r}_j$ being the position of the jth star. The physical quantities with suffix 0 are the radiation fields without extinction. The corotating flux in the azimuthal direction and the flux contributing to the radiation drag are respectively

$${\rm d}F_0^{\rm rot} = ({\rm d}E_0 + {\rm d}P_0^{\phi\phi})V_*, \tag{26}$$

$${\rm d}F_0^{\rm drag} = -({\rm d}E_0 + {\rm d}P_0^{\phi\phi})v_{\rm gas}, \tag{27}$$

where $V_* = r_*\omega$ and $v_{\rm gas} = r_{\rm gas}\omega$ are the rotational velocities of a star and a gas cloud, with r_* and $r_{\rm gas}$ being respectively the distances from the rotational axis to a star and to a gas cloud. Next, we consider the extinction by dust in clumpy gas clouds. We calculate the radiation fields by the direct integration of the radiation transfer (see Fig. 2), where the extinction by all intervening clouds from a star to a cloud is summed up. Then the radiation flux $\boldsymbol{F}$, the radiation energy density E and the radiation stress tensor P are respectively given by

$$\boldsymbol{F} = \sum_{j=1}^{N_*} \mathrm{d}\boldsymbol{F}_{0,j} \exp(-\tau_j), \tag{28}$$

$$E = \sum_{j=1}^{N_*} \mathrm{d}E_{0,j} \exp(-\tau_j), \tag{29}$$

$$P = \sum_{j=1}^{N_*} \mathrm{d}P_{0,j} \exp(-\tau_j), \tag{30}$$

where $\tau = 2\sum[1-(b/r_\mathrm{c})^2]^{1/2}\bar{\tau}$ is the optical depth for all intervening clouds along the light ray.

5.2 Angular momentum transfer in a clumpy ISM

By substituting (26)–(30) for (5), we can evaluate the total angular momentum loss rate as

$$\dot{J} = \frac{\chi}{c}\sum_{i=1}^{N_\mathrm{c}} r_i(F_i^\mathrm{rot} - F_i^\mathrm{drag}), \tag{31}$$

where $F_i^\alpha = \sum_{j=1}^{N_*} \mathrm{d}F_{0,j}^\alpha \exp(-\tau_j)$ with α being 'rot' or 'drag', and r_i is the distance from the origin to a gas cloud. If an optically thick cloud is irradiated by the radiation, only the optically thin surface layer is subject to radiation drag (Tsuribe & Umemura 1997). Then the surface layer is stripped by the drag and simultaneously loses angular momentum. We assume here that the stripped gas falls on to a central massive object. Then, with the above angular momentum loss rate, we estimate the total mass of the dusty ISM assembled on to a central massive object which may evolve into a supermassive BH. By equation (31) and the relation $\dot{M}_\mathrm{gas}/M_\mathrm{gas} = -\dot{J}/J_0$, the BH mass M_BH is assessed as

$$M_\mathrm{BH} = \int_0^{t(m_\mathrm{l})} \dot{M}_\mathrm{gas}\,\mathrm{d}t = -\int_0^{t(m_\mathrm{l})} M_\mathrm{gas}\frac{\dot{J}}{J_0}\,\mathrm{d}t, \tag{32}$$

where $t(m_\mathrm{l})$ is the age of a star with mass m_l.

Here, we introduce $\bar{N}_\mathrm{int}$ as a measure of the clumpiness of the ISM. $\bar{N}_\mathrm{int}$ is defined by

$$\bar{N}_\mathrm{int} = n_\mathrm{c}\pi r_\mathrm{c}^2 r_\mathrm{b} \frac{3}{4} N_\mathrm{c}\left(\frac{r_\mathrm{c}}{r_\mathrm{b}}\right)^2, \tag{33}$$

where $n_\mathrm{c} = N_\mathrm{c}/\frac{4}{3}\pi r_\mathrm{b}^3$ is the number density of gas clouds. $\bar{N}_\mathrm{int}$ means the average number of gas clouds that are intersected by a light ray over a bulge radius. The degree of clumpiness is larger for smaller $\bar{N}_\mathrm{int}$, and $\bar{N}_\mathrm{int} = \infty$ corresponds to a uniform distribution. When $\bar{N}_\mathrm{int}$ and the optical depth $\bar{\tau}$ of each cloud are specified, the total optical depth τ_T is given by $\tau_\mathrm{T} = \bar{N}_\mathrm{int}\bar{\tau}$. With changing $\bar{N}_\mathrm{int}$, we investigate the relationship between the clumpiness of the ISM and the radiation drag efficiency.

In Fig. 3, for different $\bar{N}_\mathrm{int}$, we show the ratio of the resultant BH mass to the bulge mass ($M_\mathrm{BH}/M_\mathrm{bulge}$) against the total optical depth τ_T. In this figure, the dashed line is the analytic solution for a uniform ISM corresponding to $\bar{N}_\mathrm{int} = \infty$, i.e. equation (24). The solid lines show the numerical results for a clumpy ISM, where the arrows represent $\bar{\tau} = 1$ for different $\bar{N}_\mathrm{int}$. The thick lines show the results for $\bar{N}_\mathrm{int} \geq 1$ and the thin lines are those for $\bar{N}_\mathrm{int} < 1$. In Fig. 3, several points are clear regarding the effects of the clumpiness on the radiation drag efficiency. First, if $\bar{N}_\mathrm{int} < 1$, the drag efficiency is saturated when $\bar{\tau} > 1$. Since the ISM is highly clumpy in this case, the radiation from distant sources which have different velocities from the absorbing clouds can contribute to the radiation drag even if $\tau_\mathrm{T} \gg 1$. However, the covering factor of clouds is smaller than unity, and therefore a large fraction of photons escape from the bulge without intersecting clouds. The saturation is attributed to these two effects. Secondly, if $\bar{N}_\mathrm{int} \approx O(1)$, $M_\mathrm{BH}/M_\mathrm{bulge}$ grows with τ_T and maintains a high level in an optically thick ISM. Obviously, the behaviour in the thick limit is different from the uniform case, although the situation is the same as the uniform case in that almost all of photons are consumed inside the bulge. This is again because the clumpiness increases the mean free paths of photons, so that the radiation from distant sources enhances the drag efficiency. Thirdly, when $\bar{N}_\mathrm{int}$ is much larger than unity, the distribution of the ISM is closer to a uniform distribution and therefore the difference between the velocity of a star and the velocity of an absorbing cloud is closer to zero, so that the drag efficiency falls as in the uniform case. To conclude, the combined effects of the high clumpiness of the ISM and the large covering factor of clouds are necessary for high drag efficiency.

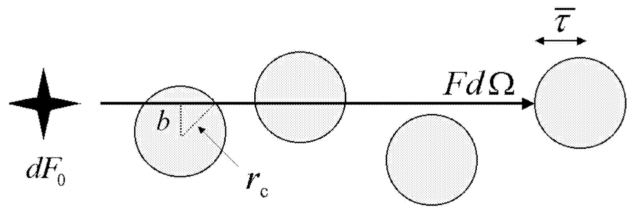

Figure 2. A schematic illustration of the radiative transfer calculations in a clumpy ISM. b and r_c are respectively the impact parameter and the radius of the clumpy gas clouds. $\bar{\tau}$ is the optical depth of a cloud.

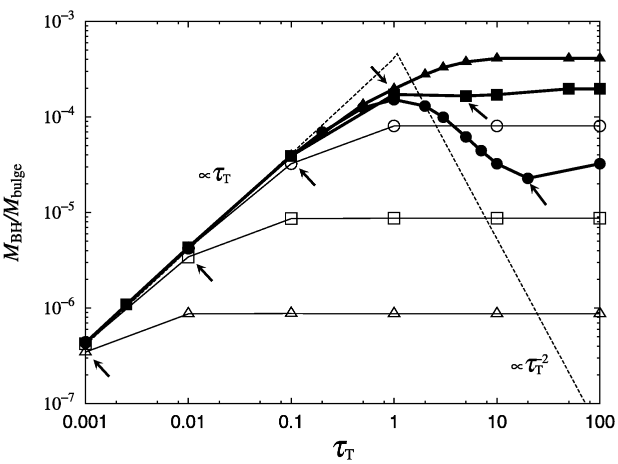

Figure 3. The BH-to-bulge mass ratio ($M_\mathrm{BH}/M_\mathrm{bulge}$) against the total optical depth (τ_T) of the bulge. The thick lines show the results for $\bar{N}_\mathrm{int} \geq 1$ and the thin lines are those for $\bar{N}_\mathrm{int} < 1$. Filled circles denote $\bar{N}_\mathrm{int} = 20$, filled squares $\bar{N}_\mathrm{int} = 5$, filled triangles $\bar{N}_\mathrm{int} = 1$, open circles $\bar{N}_\mathrm{int} = 0.1$, open squares $\bar{N}_\mathrm{int} = 0.01$, and open triangles $\bar{N}_\mathrm{int} = 0.001$. The dashed line is the analytic solution for a uniform ISM corresponding to $\bar{N}_\mathrm{int} \to \infty$, where $M_\mathrm{BH}M_\mathrm{bulge} \propto \tau_\mathrm{T}$ in an optically thin regime and $M_\mathrm{BH}M_\mathrm{bulge} \propto \tau_\mathrm{T}^{-2}$ in an optically thick regime. The arrows show the points where the optical depth of a cloud ($\bar{\tau}$) is unity. For $\bar{N}_\mathrm{int} \approx 1$, the radiation drag efficiency is maximal if $\bar{\tau} \geq 1$. For $\bar{N}_\mathrm{int} < 1$, the radiation drag efficiency is saturated when $\bar{\tau} \geq 1$.

6 BLACK HOLE-TO-BULGE MASS RATIO

The linear relation between the BH mass and the bulge mass is a direct consequence of the present radiation hydrodynamical mechanism. The possible mass accreted by the radiation drag is given by $M_{\max} = \int_0^{t(m_l)} L_{\mathrm{bulge}}(t)/c^2\,\mathrm{d}t$. Incorporating stellar evolution based on the present single-starburst model, we find $M_{\max} = 1.2\times10^{-3} M_{\mathrm{bulge}}$. As shown above, the drag efficiency is sensitively dependent on the density distributions of the ISM. In a highly clumpy ISM where $\bar{N}_{\mathrm{int}}$ is smaller than a few, the BH-to-bulge mass ratio $M_{\mathrm{BH}}/M_{\mathrm{bulge}}$ can be expressed by

$$\frac{M_{\mathrm{BH}}}{M_{\mathrm{bulge}}} = \eta \frac{M_{\max}}{M_{\mathrm{bulge}}}(1 - \mathrm{e}^{-\tau_{\mathrm{T}}}) \tag{34}$$

$$= 1.2\times10^{-3}\eta(1 - \mathrm{e}^{-\tau_{\mathrm{T}}}), \tag{35}$$

where η gives the radiation drag efficiency. From the above analysis, η is found to be maximally 0.34 in the optically thick limit, and then $M_{\mathrm{BH}}/M_{\mathrm{bulge}} = 4.1\times10^{-4}$.

The present model may be too simple in some respects to compare the results closely with observations. For a more precise prediction of $M_{\mathrm{BH}}/M_{\mathrm{bulge}}$, it seems necessary to consider further effects which have not been incorporated in this simple model. In the present analysis, we assumed an initial coeval event of star formation, and subsequent passive evolution without further star formation episodes. The radiation drag efficiency is basically determined by the total number of photons which are emitted from sources and absorbed by clouds during the whole history of the bulge. The recycling of the ISM for star formation generates more photons and therefore could enhance the mass ratio roughly by a factor of 2 (Umemura 2001). Also, in realistic situations, the radiation drag is not likely to remove completely the angular momentum of stripped gas, and also stripped gas may be mixed with ISM having appreciable angular momentum. Although the detailed processes are not very clear at present, a little leftover angular momentum may lead to the formation of a viscous accretion disc around a BH, which could ignite QSO activity with nearly Eddington luminosity (Umemura 2001). If QSO activity is triggered, the radiation from the QSO can also exert the drag force. This effect can enhance the mass ratio by maximally a factor of 1.7 (Umemura 2001). Furthermore, if a galactic wind occurs, it might cause a transition from an optically thick starburst phase to an optically thin QSO phase, and simultaneously reduce the drag efficiency.

If the above effects are taken into account, the mass ratio could be maximally $M_{\mathrm{BH}}/M_{\mathrm{bulge}} = 1.4\times10^{-3}$. This is compared with recent observational data in Fig. 4, combined with the result of a single-starburst model, $M_{\mathrm{BH}}/M_{\mathrm{bulge}} = 4.1\times10^{-4}$. In Fig. 4, the hatched area is the prediction of the present analysis. As seen in this figure, the present radiation hydrodynamical model can roughly account for the observational data, although the prediction falls slightly short of the observed median mass ratio. The prediction is smaller by a factor of 6 than $\langle M_{\mathrm{BH}}/M_{\mathrm{bulge}}\rangle = 0.006$ by Magorrian et al. (1998), while it is comparable to $\langle M_{\mathrm{BH}}/M_{\mathrm{bulge}}\rangle = 0.001$ by Merritt & Ferrarese (2001a).

Another important effect is the geometrical dilution. In previous works, the radiation drag efficiency would be strongly subject to the effects of geometry (Umemura et al. 1997, 1998; Ohsuga et al. 1999). A large fraction of emitted photons can escape from a disc-like system and thus the radiation drag efficiency is considerably reduced. Recent observations have revealed that the BH mass fraction is significantly smaller than 0.001 in disc galaxies (Salucci et al. 2000; Sarzi et al. 2001). Geometrical dilution may be a reason for the observational fact in disc galaxies, but the quantitative details are not clear before such an aspherical system is actually simulated.

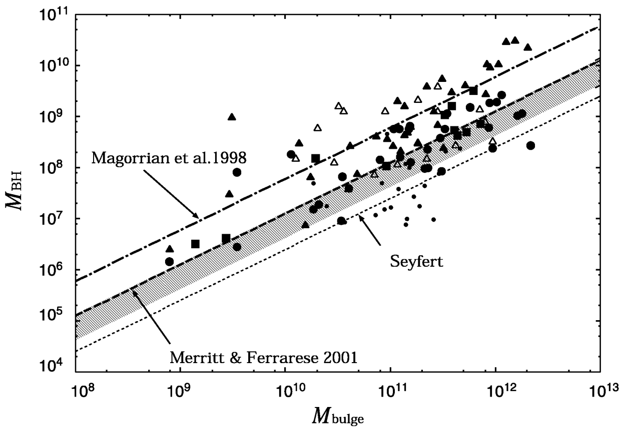

Figure 4. The relation between the BH mass and the bulge mass. The vertical axis is the BH mass, and the horizontal axis is the bulge mass, in units of $\mathrm{M}_{\odot}$. Recent observational results are plotted by symbols. The filled triangles denote elliptical galaxies from Magorrian et al. (1998). The filled squares show elliptical galaxies from Ho (1999), Ferrarese & Merritt (2000), Kormendy & Ho (2000) and Sarzi et al. (2001). The filled circles denote elliptical galaxies from Merritt & Ferrarese (2001a). The small dots denote Seyfert galaxies from Ho (1999), Wandel (1999), and Gebhardt et al. (2000b), and the open triangles show QSOs from Laor (1998). The relation of Magorrian et al. (1998) is $M_{\mathrm{BH}} = 0.006 M_{\mathrm{bulge}}$, which is shown by a dot-dashed line; the relation of Merritt & Ferrarese (2001a) is $M_{\mathrm{BH}} = 0.001 M_{\mathrm{bulge}}$, which is shown by a dashed line; and the relation for Seyfert galaxies is $M_{\mathrm{BH}} = 2.5\times10^{-4} M_{\mathrm{bulge}}$ (Sarzi et al. 2001), which is shown by a thin dashed line. The hatched area shows the prediction of this paper. The lower bound is a single-starburst model ($M_{\mathrm{BH}} = 4.1\times10^{-4} M_{\mathrm{bulge}}$). The upper bound is the model incorporating the effect of the recycling of star formation and AGN activity ($M_{\mathrm{BH}} = 1.4\times10^{-3} M_{\mathrm{bulge}}$).

7 CONCLUSIONS

By assuming a simple model of a bulge, we have investigated the mutual effect between the clumpiness of the interstellar medium and the optical depth on the radiation drag efficiency for angular momentum transfer. In a clumpy ISM, we have accurately solved 3D radiation transfer to calculate the radiation drag force by the rotating bulge stars. We find that the radiation drag efficiency is sensitively dependent on the density distribution of the ISM in an optically thick regime. The efficiency drops by a factor of τ_{T}^{-2} in a uniform ISM, while the efficiency turns out to be almost constant at a high level in a clumpy ISM. Also, the radiation drag efficiency falls as the covering factor of clouds becomes smaller than unity. Hence, for the radiation drag to work effectively, it is necessary that the covering factor be larger than unity and that the distribution of the ISM be highly clumpy. The present radiation hydrodynamical mechanism accounts for the linear relation between the mass of a supermassive black hole and the mass of a galactic bulge. The range of predicted mass ratio is from $M_{\mathrm{BH}}/M_{\mathrm{bulge}} = 4.1\times10^{-4}$ to 1.4×10^{-3}. Although we have adopted a highly simplified model, the result roughly accounts for recent observational trends. Thus it seems that more elaborate calculations deserve to be performed in the present context. In the future, we should consider further several effects that have not been incorporated in the present analysis, and which can influence the mass ratio significantly: e.g. realistic chemical evolution and geometrical dilution.

ACKNOWLEDGMENTS

We thank M. Mori, T. Nakamoto and H. Susa for helpful discussions. We are grateful to M. Hayashi and K. Ohsuga for many useful comments. We also thank the anonymous referee for valuable comments. Numerical simulations were performed with facilities at the Centre for Computational Physics, University of Tsukuba. This work was supported in part by a Grant-in-Aid of the JSPS, 11640225.

REFERENCES

Adams F. C., Graff D. S., Richstone D., 2001, ApJ, 551, L31
Arimoto N., Yoshii Y., 1986, A&A, 164, 260
Barns J., Efstathiou G., 1987, ApJ, 319, 575
Brandl B., Brandner W., Eisenhauer F., Moffat A. F. J., Palla F., Zinnecher H., 1999, A&A, 352, L69
Charlot S., Ferrari F., Mathews G. J., Silk J., 1993, ApJ, 419, L57
Doane J. S., Mathews W. G., 1993, ApJ, 419, 573
Doyon R., Puxley P. J., Joseph R. D., 1992, ApJ, 397, 117
Ferrarese L., Merritt D., 2000, ApJ, 539, L9
Ferrarese L., Pogge R. W., Peterson B. M., Merritt D., Wandel A., Joseph C. L., 2001, ApJ, 555, L79
Fukue J., Umemura M., Mineshige S., 1997, PASJ, 49, 673
Gebhardt K. et al., 2000a, ApJ, 539, L13
Gebhardt K. et al., 2000b, ApJ, 543, L5
Gordon K., Calzetti D., Witt A. N., 1997, ApJ, 487, 625
Heavens A., Peacock J., 1988, MNRAS, 232, 339
Hill J. K., Isensee J. E., Cornett R. H., Bohlin R. C., O'Connell R. W., Roberts M. S., Smith A. M., Stecher T. P., 1994, ApJ, 425, 122
Ho L. C., 1999, in Chakrabarti S. K., ed., Observational Evidence for Black Holes In the Universe. Dordrecht, Kluwer, p. 157
Kodama T., Arimoto N., 1997, A&A, 320, 41
Kormendy J., Ho L. C., 2000, Encyclopedia of Astronomy and Astrophysics
Kormendy J., Richstone D., 1995, ARA&A, 33, 581
Lang K. R., 1974, Astrophysical Data: Planets and Stars. Springer-Verlag, Berlin
Laor A., 1998, ApJ, 505, L83
McLure R. J., Dunlop J. S., 2001a, MNRAS, submitted
McLure R. J., Dunlop J. S., 2001b, MNRAS, 327, 199
Magorrian J. et al., 1998, ApJ, 115, 2285
Merrifield M. R., Forbes D. A., Terlevich A. I., 2000, MNRAS, 313, L29
Merritt D., Ferrarese L., 2001a, MNRAS, 320, L30
Merritt D., Ferrarese L., 2001b, ApJ, 547, 140
Mihalas D., Mihalas B. W., 1984, Foundations of Radiation Hydrodynamics. Oxford Univ. Press, Oxford, section 7
Miyoshi M., Morton J., Herrnstein J., Greenhill L., Nakai N., Diamond P., Inoue M., 1995, Nat, 373, 127
Mori M., Yoshii Y., Tsujimoto T., Nomoto K., 1997, ApJ, 478, L21
Nelson C. H., 2000, ApJ, 544, L91
Ohsuga K., Umemura M., Fukue J., Mineshige S., 1999, PASJ, 51, 345
Ostriker J. P., 2000, Phys. Rev. Lett., 84, 5258
Richstone D. et al., 1998, Nat, 395A, 14
Salucci P., Ratnam C., Monaco P., Danse L., 2000, MNRAS, 317, 488
Sanders D. B., Soifer B. T., Elias J. H., Madore B. F., Matthews K., Neugebauer G., Scoville N. Z., 1988, ApJ, 325, 74
Sarzi M., Rix H.-W., Shields C., Rudnick G., Ho L. C., McIntosh D. H., Filippenko A. V., Sargent W. L. W., 2001, ApJ, 550, 65
Selman F., Melnick J., Bosch G., Terlevich R., 1999, A&A, 347, 532
Silk J., Rees M. J., 1998, A&A, 331, L1
Tsuribe T., Umemura M., 1997, ApJ, 486, 48
Umemura M., 2001, ApJL, 560, L29
Umemura M., Fukue J., Mineshige S., 1997, ApJ, 479, L97
Umemura M., Fukue J., Mineshige S., 1998, MNRAS, 299, 1123
Wandel A., 1999, ApJ, 519, L39
Wandel A., 2001ApJ,, preprint (astro-ph/0108461)
Yoshii Y., Arimoto N., 1987, A&A, 188, 13

This paper has been typeset from a TEX/LATEX file prepared by the author.